

Analytical solutions for spin 7/2 line intensities in solid state NMR

By S. Z. AGEEV and B. C. SANCTUARY

Department of Chemistry, McGill University, Montreal, PQ, Canada H3A 2K6

(Received 15 June 1994; revised version accepted 3 November 1994)

Developments in computer algebra have prompted us to reconsider earlier, intractable problems. Here the density matrix of spin 7/2 subject to the first order quadrupolar interaction and excited by a RF pulse is calculated ignoring rapidly oscillating terms. The results are studied for a variety of conditions which scale as the ratio of the quadrupolar coupling constant to the RF pulse amplitude. The line intensities of the central and satellite transition are also investigated.

1. Introduction

Since the seminal work of Samoson and Lippmaa [1], a variety of theoretical approaches have appeared in connection with solid state NMR dealing with half integer spins subject to a first order quadrupolar interaction. Spin 3/2 has received the most attention [2–8]. For spin 5/2 attempts to extract structural and dynamical information have been made [4, 9]. Recently, Man [10] has extended the analytical calculations from spin 3/2 to spin 5/2. That is, while the pulse is on, the first order quadrupole is retained. He also treated Solomon echoes of a spin 5/2 under the same conditions [11]. In the present paper, the density matrix and spin 7/2 line intensities after a single RF pulse are calculated. The results suggest simple experiments for obtaining line intensities as functions of RF pulse length which can be used to determine the amplitude of the first order quadrupolar interaction [10].

2. Theoretical consideration

The Hamiltonian for the problem in question is

$$H = \hbar(-\omega_0 I_z + H_Q^{(1)} - 2\omega_1 \cos(\omega t - \phi) I_x), \quad (1)$$

where ω_0 is the Larmor frequency of the central transition, and

$$H_Q^{(1)} = \frac{1}{3}\omega_Q[3I_z^2 - I(I+1)]$$

with

$$\omega_Q = \frac{3e^2qQ}{8I(2I-1)} (3 \cos^2 \beta - 1 + \eta \sin^2 \beta \cos 2\alpha)$$

$H_Q^{(1)}$ is the first order quadrupolar Hamiltonian. Euler angles α and β describe the strong static magnetic field with respect to the quadrupole principal axis system (QPAS). The RF amplitude ω_1 , the carrier frequency ω , and the phase ϕ describe a pulse. Transforming into the rotating frame associated with the central transition and neglecting the offset and high frequency terms results in

$$\tilde{H}/\hbar = H_Q^{(1)} + \omega_1 I_x, \quad (2)$$

where we assume that $\phi = \pi$.

The dynamics of the spin 7/2 system under a pulse along the negative x-axis (i.e., $\phi = \pi$) is described by the density matrix

$$\rho(t) = \exp(-i\tilde{H}t/\hbar)\rho(0)\exp(i\tilde{H}t/\hbar), \tag{3}$$

with the initial condition $\rho(0) = I_z$.

The matrix representation of \tilde{H} is given in table 1. It can be diagonalized by a two step procedure described elsewhere [1, 10]. The transformation A_1 brings Hamiltonian (2) to the block-diagonal form $H_{A_1} = A_1\tilde{H}A_1$ (table 1) where each block is a 4×4 symmetric matrix. The eight eigenvalues of H_{A_1} , given by the solution of two fourth-order equations, are

$$\left. \begin{aligned} E_{11} &= (R_1 + D_1)/2 - \omega_1/2 & E_{21} &= (R_2 + D_2)/2 + \omega_1/2 \\ E_{12} &= (R_1 - D_1)/2 - \omega_1/2 & E_{22} &= (R_2 - D_2)/2 + \omega_1/2 \\ E_{13} &= -(R_1 - S_1)/2 - \omega_1/2 & E_{23} &= -(R_2 - S_2)/2 + \omega_1/2 \\ E_{14} &= -(R_1 + S_1)/2 - \omega_1/2 & E_{14} &= -(R_2 + S_2)/2 + \omega_1/2. \end{aligned} \right\} \tag{4}$$

where

$$D_{1,2} = \left[\frac{1}{2} \left(X_{1,2} + \frac{Y_{1,2}}{R_{1,2}} \right) - R_{1,2}^2 \right]^{1/2}$$

and

$$S_{1,2} = \left[\frac{1}{2} \left(X_{1,2} - \frac{Y_{1,2}}{R_{1,2}} \right) - R_{1,2}^2 \right]^{1/2},$$

in which

$$R_{1,2} = \frac{1}{\sqrt{6}} [X_{1,2} + (X_{1,2}^2 + 12Z_{1,2})^{1/2} \cos(\beta_{12}/3)]^{1/2}$$

with

$$\cos(\beta_{12}) = -[X_{1,2}^3 - 36X_{1,2}Z_{1,2} - 54Y_{1,2}^2]/(X_{1,2}^2 + 12Z_{1,2})^{3/2}.$$

The values X , Y and Z depend on the interaction parameters of Hamiltonian (2) as

$$\left. \begin{aligned} X_{1,2} &= 4(\pm 10\omega_Q\omega_1 + 42\omega_Q^2 + 10\omega_1^2) \\ Y_{1,2} &= 4(\mp 8\omega_Q^2\omega_1 - 32\omega_Q\omega_1^2 + 64\omega_Q^3) \\ Z_{1,2} &= 16(105\omega_Q^4 + 9\omega_1^4 \pm 74\omega_Q^3\omega_1 + 59\omega_Q^2\omega_1^2 \pm 18\omega_Q\omega_1^3). \end{aligned} \right\} \tag{5}$$

The subscripts 1 and 2 refer to the upper (4×4) block and lower block, respectively. Moreover, the upper signs in expression (5) refer to block 1 and the lower signs refer to block 2. We have put $\hbar = 1$ (frequency units), for convenience.

The components of the normalized eigenvectors associated with these eight eigenvalues are

$$\begin{aligned} X_{1i} &= -\frac{A}{7\omega_Q - E_{1i}} \bigg/ Q_{1i} \\ Y_{1i} &= 1/Q_{1i} \\ Z_{1i} &= \frac{1}{B} \left(\frac{A^2}{7\omega_Q - E_{1i}} - (\omega_Q - E_{1i}) \right) \bigg/ Q_{1i} \end{aligned}$$

Table 1. The matrix representation of \tilde{H}/\hbar , A_1 and H_{A_1}/\hbar .

$\frac{\tilde{H}}{\hbar} =$	$\begin{bmatrix} 7\omega_Q & \frac{\sqrt{7}}{2}\omega_1 & 0 & 0 & 0 & 0 & 0 & 0 \\ \frac{\sqrt{7}}{2}\omega_1 & \omega_Q & \sqrt{3}\omega_1 & 0 & 0 & 0 & 0 & 0 \\ 0 & \sqrt{3}\omega_1 & -3\omega_Q & \frac{(15)^{1/2}}{2}\omega_1 & 0 & 0 & 0 & 0 \\ 0 & 0 & \frac{(15)^{1/2}}{2}\omega_1 & -5\omega_Q & 2\omega_1 & 0 & 0 & 0 \\ 0 & 0 & 0 & 2\omega_1 & -5\omega_Q & \frac{(15)^{1/2}}{2}\omega_1 & 0 & 0 \\ 0 & 0 & 0 & 0 & \frac{(15)^{1/2}}{2}\omega_1 & -3\omega_Q & \sqrt{3}\omega_1 & 0 \\ 0 & 0 & 0 & 0 & 0 & \sqrt{3}\omega_1 & \omega_Q & \frac{\sqrt{7}}{2}\omega_1 \\ 0 & 0 & 0 & 0 & 0 & 0 & \frac{\sqrt{7}}{2}\omega_1 & 7\omega_Q \end{bmatrix}$
$A_1 = \frac{\sqrt{2}}{2}$	$\begin{bmatrix} 1 & 0 & 0 & 0 & 0 & 0 & 0 & 1 \\ 0 & 1 & 0 & 0 & 0 & 0 & 1 & 0 \\ 0 & 0 & 1 & 0 & 0 & 1 & 0 & 0 \\ 0 & 0 & 0 & 1 & 1 & 0 & 0 & 0 \\ 0 & 0 & 0 & -1 & 1 & 0 & 0 & 0 \\ 0 & 0 & -1 & 0 & 0 & 1 & 0 & 0 \\ 0 & -1 & 0 & 0 & 0 & 0 & 1 & 0 \\ -1 & 0 & 0 & 0 & 0 & 0 & 0 & 1 \end{bmatrix}$
$\frac{H_{A_1}}{\hbar} =$	$\begin{bmatrix} 7\omega_Q & \frac{\sqrt{7}}{2}\omega_1 & 0 & 0 & 0 & 0 & 0 & 0 \\ \frac{\sqrt{7}}{2}\omega_1 & \omega_Q & \sqrt{2}\omega_1 & 0 & 0 & 0 & 0 & 0 \\ 0 & \sqrt{3}\omega_1 & -3\omega_Q & \frac{(15)^{1/2}}{2}\omega_1 & 0 & 0 & 0 & 0 \\ 0 & 0 & \frac{(15)^{1/2}}{2}\omega_1 & -5\omega_Q - 2\omega_1 & 0 & 0 & 0 & 0 \\ 0 & 0 & 0 & 0 & -5\omega_Q + 2\omega_1 & \frac{(15)^{1/2}}{2}\omega_1 & 0 & 0 \\ 0 & 0 & 0 & 0 & \frac{(15)^{1/2}}{2}\omega_1 & -3\omega_Q & \sqrt{3}\omega_1 & 0 \\ 0 & 0 & 0 & 0 & 0 & \sqrt{3}\omega_1 & \omega_Q & \frac{\sqrt{7}}{2}\omega_1 \\ 0 & 0 & 0 & 0 & 0 & 0 & \frac{\sqrt{7}}{2}\omega_1 & 7\omega_Q \end{bmatrix}$

$$\begin{aligned}
 T_{1i} &= \frac{C}{B(5\omega_Q + 2\omega_1 + E_{1i})} \left(\frac{A^2}{7\omega_Q - E_{1i}} - (\omega_Q - E_{1i}) \right) / Q_{1i} \\
 X_{2i} &= -\frac{C}{-5\omega_Q + 2\omega_1 - E_{2i}} / Q_{2i} \\
 Y_{2i} &= 1/Q_{2i} \\
 Z_{2i} &= \frac{1}{B} \left(\frac{C^2}{-5\omega_Q + 2\omega_1 - E_{2i}} + 3\omega_Q + E_{2i} \right) / Q_{2i} \\
 T_{2i} &= -\frac{A}{B(7\omega_Q - E_{2i})} \left(\frac{C^2}{-5\omega_Q + 2\omega_1 - E_{2i}} + 3\omega_Q + E_{2i} \right) / Q_{2i},
 \end{aligned}$$

where $i = 1, 2, 3$ and 4 , the values Q_{1i} and Q_{2i} are chosen to normalize each eigenvector and

$$A = \frac{\sqrt{7}}{2} \omega_1, \quad B = \sqrt{3} \omega_1, \quad C = \frac{(15)^{1/2}}{2} \omega_1.$$

The transformation matrix which diagonalizes H_{A_1} and the matrix of eigenvalues are

$$T = \begin{pmatrix} P_1 & 0 \\ 0 & P_2 \end{pmatrix}, \quad E = \begin{pmatrix} E_1 & 0 \\ 0 & E_2 \end{pmatrix}, \tag{6}$$

where the corresponding blocks are defined in table 2. The equation for the density matrix (3) becomes

$$\rho(t) = A_1 T \exp(-iEt)(A_1 T)^{\dagger} I_z A_1 T \exp(iEt)(A_1 T)^{\dagger}. \tag{7}$$

The calculation of the density matrix components was performed using ‘Maple’ for UNIX on a SUN SparcStation. The results are given in table 3. From these one can determine the line intensities of the central and four satellite lines.

The total line intensity is given by

$$F = \langle I_y \rangle = \text{tr} \{ \rho(t) I_y \}. \tag{8}$$

Table 2. The submatrices in equation (6).

$ P_1 = \begin{pmatrix} X_{11} & X_{12} & X_{13} & X_{14} \\ Y_{11} & Y_{12} & Y_{13} & Y_{14} \\ Z_{11} & Z_{12} & Z_{13} & Z_{14} \\ T_{11} & T_{12} & T_{13} & T_{14} \end{pmatrix} $	$ P_2 = \begin{pmatrix} X_{21} & X_{22} & X_{23} & X_{24} \\ Y_{21} & Y_{22} & Y_{23} & Y_{24} \\ Z_{21} & Z_{22} & Z_{23} & Z_{24} \\ T_{21} & T_{22} & T_{23} & T_{24} \end{pmatrix} $
$ E_1 = \begin{pmatrix} E_{11} & 0 & 0 & 0 \\ 0 & E_{12} & 0 & 0 \\ 0 & 0 & E_{13} & 0 \\ 0 & 0 & 0 & E_{14} \end{pmatrix} $	$ E_2 = \begin{pmatrix} E_{21} & 0 & 0 & 0 \\ 0 & E_{22} & 0 & 0 \\ 0 & 0 & E_{23} & 0 \\ 0 & 0 & 0 & E_{24} \end{pmatrix} $

Table 3. The components of the density matrix $\rho(t)$ (equation (7)). It is assumed here that each term has to be multiplied by $L_{ij}/4$ and summed over i and j . Because the density matrix is Hermitian, only its lower triangle is reported.

$\rho_{11} = 2X_{1i}T_{2j} \cos \omega_{ij}t$				
$\rho_{21} = X_{1i}Z_{2j} \exp(i\omega_{ij}t) + Y_{1i}T_{2j} \exp(-i\omega_{ij}t)$	$\rho_{22} = 2Y_{1i}Z_{2j} \cos \omega_{ij}t$			
$\rho_{31} = X_{1i}Y_{2j} \exp(i\omega_{ij}t) + Z_{1i}T_{2j} \exp(-i\omega_{ij}t)$	$\rho_{32} = Y_{1i}Y_{2j} \exp(i\omega_{ij}t) + Z_{1i}Z_{2j} \exp(-i\omega_{ij}t)$			
$\rho_{33} = 2Z_{1i}Y_{2j} \cos \omega_{ij}t$				
$\rho_{41} = X_{1i}X_{2j} \exp(i\omega_{ij}t) + T_{1i}T_{2j} \exp(-i\omega_{ij}t)$	$\rho_{42} = Y_{1i}X_{2j} \exp(i\omega_{ij}t) + T_{1i}Z_{2j} \exp(-i\omega_{ij}t)$			
$\rho_{43} = Z_{1i}X_{2j} \exp(i\omega_{ij}t) + T_{1i}Y_{2j} \exp(-i\omega_{ij}t)$	$\rho_{44} = 2T_{1i}X_{2j} \cos \omega_{ij}t$			
$\rho_{51} = X_{1i}X_{2j} \exp(i\omega_{ij}t) - T_{1i}T_{2j} \exp(-i\omega_{ij}t)$	$\rho_{52} = Y_{1i}X_{2j} \exp(i\omega_{ij}t) - T_{1i}Z_{2j} \exp(-i\omega_{ij}t)$			
$\rho_{53} = Z_{1i}X_{2j} \exp(i\omega_{ij}t) - T_{1i}Y_{2j} \exp(-i\omega_{ij}t)$	$\rho_{54} = 2iT_{1i}X_{2j} \sin \omega_{ij}t$			
$\rho_{55} = -\rho_{44}$				
$\rho_{61} = X_{1i}Y_{2j} \exp(i\omega_{ij}t) - Z_{1i}T_{2j} \exp(-i\omega_{ij}t)$	$\rho_{62} = Y_{1i}Y_{2j} \exp(i\omega_{ij}t) - Z_{1i}Z_{2j} \exp(-i\omega_{ij}t)$			
$\rho_{63} = 2iZ_{1i}Y_{2j} \sin \omega_{ij}t$				
$\rho_{71} = X_{1i}Z_{2j} \exp(i\omega_{ij}t) - Y_{1i}T_{2j} \exp(-i\omega_{ij}t)$	$\rho_{72} = 2iY_{1i}Z_{2j} \sin \omega_{ij}t$			
$\rho_{81} = 2iX_{1i}T_{2j} \sin \omega_{ij}t$				
$\rho_{64} = -\rho_{53}^*$	$\rho_{65} = -\rho_{43}^*$	$\rho_{66} = -\rho_{33}$		
$\rho_{73} = -\rho_{62}^*$	$\rho_{74} = -\rho_{52}^*$	$\rho_{75} = -\rho_{42}^*$	$\rho_{76} = -\rho_{32}^*$	$\rho_{77} = -\rho_{22}$
$\rho_{82} = -\rho_{71}^*$	$\rho_{83} = -\rho_{61}^*$	$\rho_{83} = -\rho_{61}^*$	$\rho_{84} = -\rho_{51}^*$	$\rho_{85} = -\rho_{41}^*$
$\rho_{86} = -\rho_{51}^*$	$\rho_{87} = -\rho_{21}^*$	$\rho_{88} = -\rho_{11}$		

Following [12], the intensities of the various lines can be obtained using the operators I_y^{lm} where

$$I_y = \sqrt{7}(I_y^{12} + I_y^{78}) + 2\sqrt{3}(I_y^{23} + I_y^{67}) + (15)^{1/2}(I_y^{34} + I_y^{56}) + 4I_y^{45}, \quad (9)$$

and l, m take values from 1 to 8. Hence the intensity of the central line is

$$\begin{aligned} F^{45}(t) &= \text{tr}(\rho(t)4I_y^{45}) \\ &= 2 \sum_{i,j=1}^4 L_{ij}T_{1i}X_{2j} \sin \omega_{ij}t, \end{aligned} \quad (10)$$

where

$$L_{ij} = 7X_{1i}T_{2j} + 5Y_{1i}Z_{2j} + 3Z_{1i}Y_{2j} + T_{1i}X_{2j}.$$

The nutation frequencies ω_{ij} are defined as

$$\omega_{ij} = E_{1i} - E_{2j}.$$

Note that the sums run over i and j from 1 to 4 only. Referring to table 2, the energies associated with the upper block are E_{1i} and those of the lower block are E_{2j} so each block has 4 energies. The operators I_y^{lm} couple elements only between the upper and lower blocks.

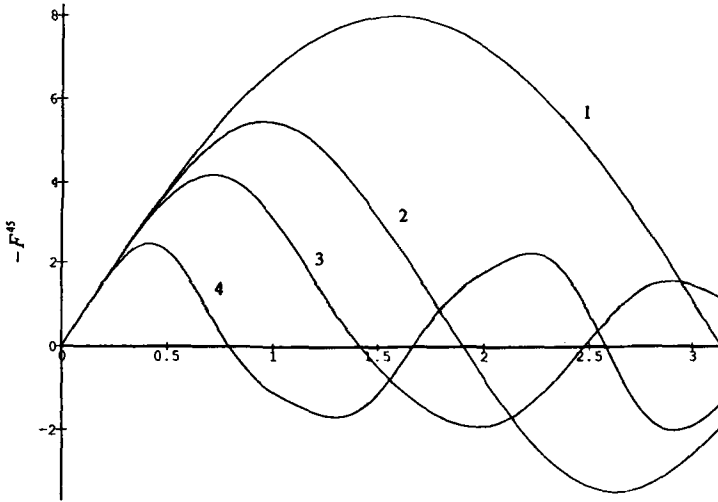


Figure 1. The intensity of the central line F^{45} as a function of the RF pulse length in units of $1/\omega_1$ for: 1, $\omega_Q/\omega_1 = 0$; 2, $\omega_Q/\omega_1 = 0.5$; 3, $\omega_Q/\omega_1 = 1$; and 4, $\omega_Q/\omega_1 = 3.5$.

In a similar way the corresponding intensity of the first inner satellite line is

$$F^{34} = \frac{(15)^{1/2}}{4} \sum_{i,j=1}^4 L_{ij}(Z_{1i}X_{2j} - T_{1i}Y_{2j}) \sin \omega_{ij}t \tag{11}$$

while that of the second inner satellite line is

$$F^{23} = -\frac{\sqrt{3}}{2} \sum_{i,j=1}^4 L_{ij}(Z_{1i}Z_{2j} - Y_{1i}Y_{2j}) \sin \omega_{ij}t. \tag{12}$$

The intensity of the outer satellite line is

$$F^{12} = \frac{\sqrt{7}}{4} \sum_{i,j=1}^4 L_{ij}(X_{1i}Z_{2j} - Y_{1i}T_{2j}) \sin \omega_{ij}t. \tag{13}$$

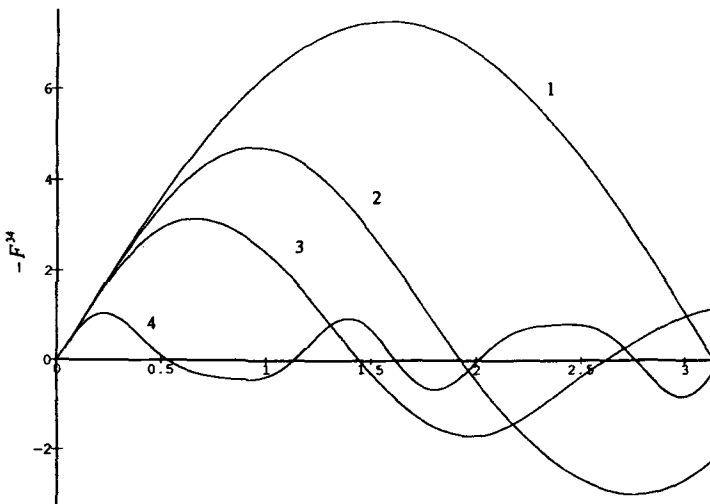


Figure 2. The intensity of the first inner line F^{34} as a function of the RF pulse length in units of $1/\omega_1$ for: 1, $\omega_Q/\omega_1 = 0$; 2, $\omega_Q/\omega_1 = 0.5$; 3, $\omega_Q/\omega_1 = 1$; and 4, $\omega_Q/\omega_1 = 3.5$.

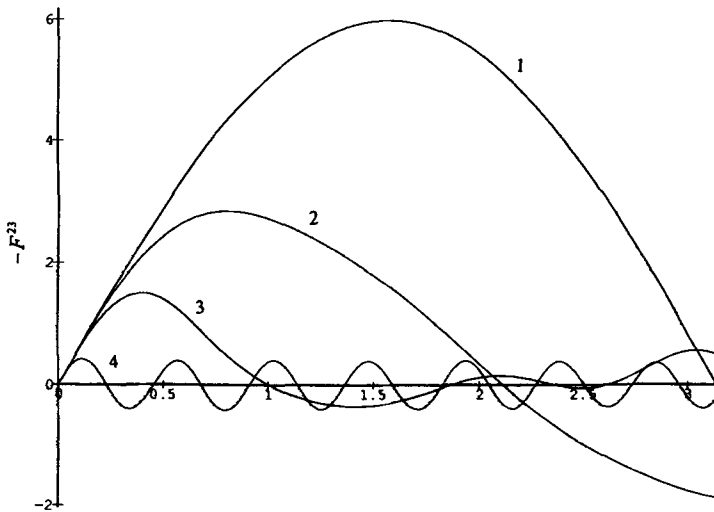


Figure 3. The intensity of the second inner line F^{23} as a function of the RF pulse length in units of $1/\omega_1$ for: 1, $\omega_Q/\omega_1 = 0$; 2, $\omega_Q/\omega_1 = 0.5$; 3, $\omega_Q/\omega_1 = 1$; and 4, $\omega_Q/\omega_1 = 3.5$.

The total line intensity for spin 7/2 is simply

$$F = F^{45} + 2F^{34} + 2F^{23} + 2F^{12}. \quad (14)$$

The line intensities are thus all sums of sixteen frequency terms, each of different amplitude. These amplitudes and frequencies vary with the relative strength of ω_Q and the ratio ω_Q/ω_1 . Figures 1-4 show the intensities of the central and satellite lines as functions of the pulse length. The intensity of the central line approaches the following limits

$$\begin{aligned} F^{45} &= -16 \sin \omega_1 t & \text{when } \omega_Q \ll \omega_1 \\ &= -4 \sin 4\omega_1 t & \text{when } \omega_Q \gg \omega_1 \end{aligned} \quad (15)$$

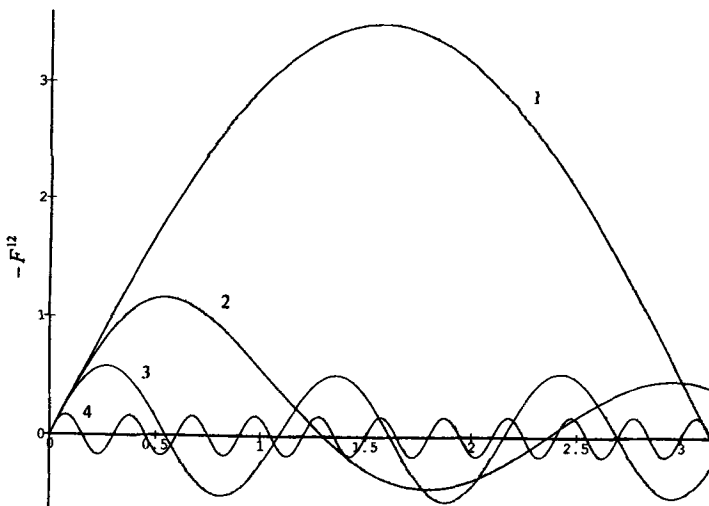


Figure 4. The intensity of the outer line F^{12} as a function of the RF pulse length in units of $1/\omega_1$ for: 1, $\omega_Q/\omega_1 = 0$; 2, $\omega_Q/\omega_1 = 0.5$; 3, $\omega_Q/\omega_1 = 1$; and 4, $\omega_Q/\omega_1 = 3.5$.

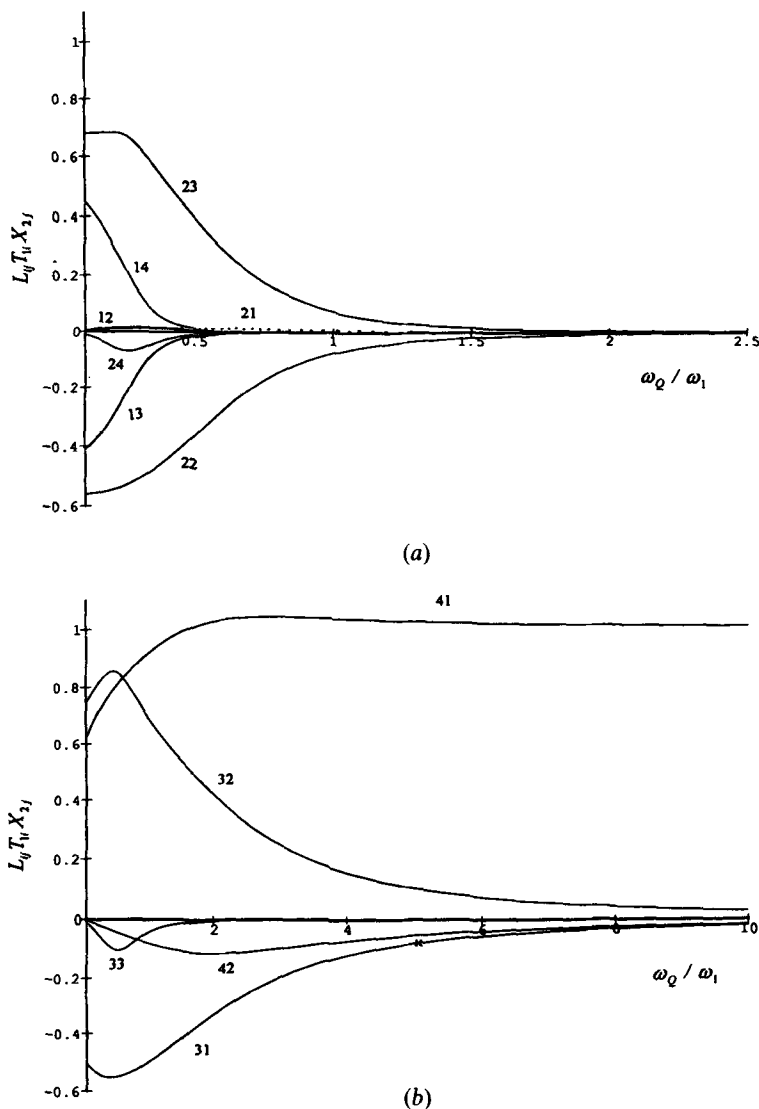


Figure 5. The sixteen amplitudes $L_{ij}T_{1i}X_{2j}$ as functions of ω_Q/ω_1 . The numbers relate to the subscripts i and j of $L_{ij}T_{1i}X_{2j}$. Only non-negligible amplitudes are shown.

which show that the amplitude and position change in agreement with [1]. The factor of $4\omega_1 t$ follows from the general treatment of selective pulses where

$$\omega_{1\text{eff}} = [I(I+1) - M(M+1)]^{1/2}\omega_1$$

with $I = 7/2$ and $M = -1/2$ [13].

There is a region in figure 1 for $t \leq (0.25/\omega_1)$ where the intensity of the central transition is a linear function of the pulse length. This is useful for treating powders [10]. The other line intensity decreases to zero when ω_Q increases and does not show similar linear regions, in contrast to the situation for the central transition.

Equations (10)–(13) can be investigated in the frequency domain. The Fourier transform of these give sets of sixteen lines located at ω_{ij} . The amplitudes of these

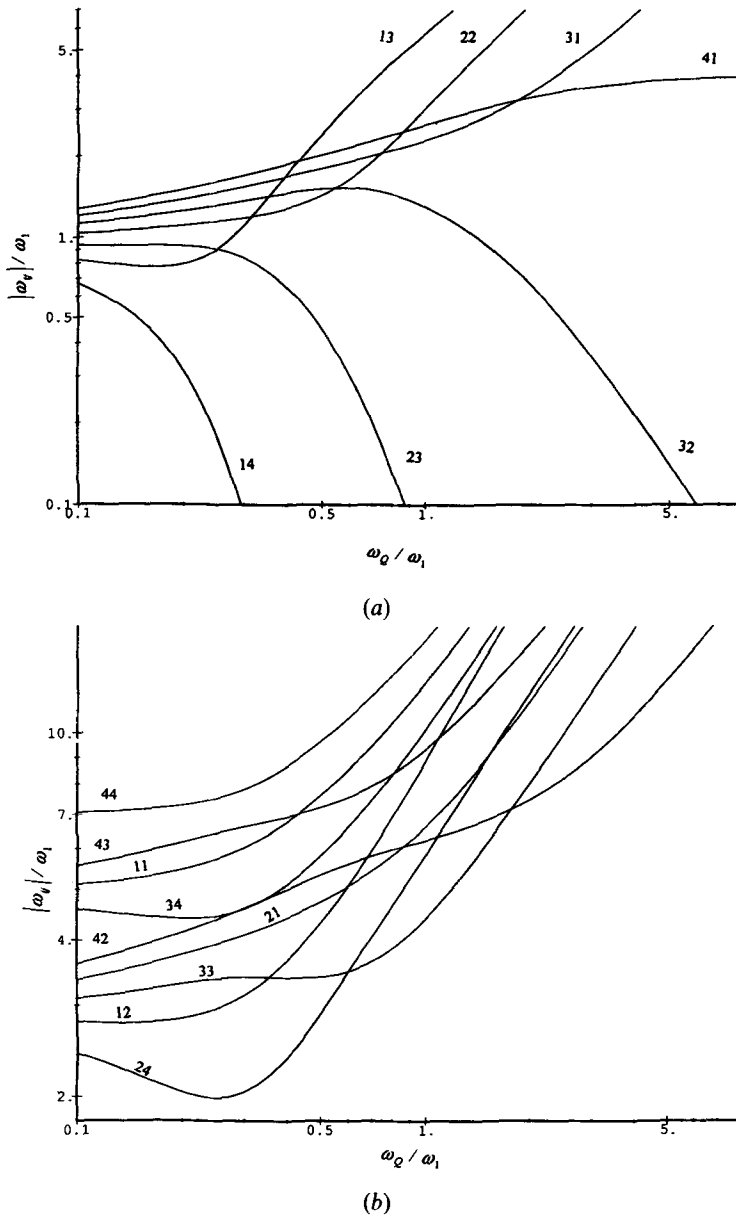


Figure 6. Log-log plots of the frequencies $|\omega_{ij}|/\omega_1$ as the functions of ω_Q/ω_1 . The numbers relate to the subscripts i and j of $|\omega_{ij}|/\omega_1$.

lines are seen in equations (8)–(11) and vary depending on the ratio ω_Q/ω_1 . For example, for the central transition, the amplitudes $L_{ij}T_{1i}X_{2j}$ are shown in figure 5 as functions of ω_Q/ω_1 . These demonstrate the relative importance of the various contributions from the nutation frequencies. For example, for $(\omega_Q/\omega_1) \rightarrow \infty$ only one is relevant, as expected, whereas for $\omega_Q/\omega_1 \leq 0.5$ all but seven are negligible. To relate to the previous work [1, 10], figure 6 shows log-log plots of $|\omega_{ij}|/\omega_1$ versus $\omega_Q/\omega_1 \leq 0.5$ the seven non-negligible lines are located near ω_1 . As the ratio ω_Q/ω_1 increases, these plots show that some lines become less important while others become

more important. Eventually for $\omega_Q/\omega_1 \geq 10$ only one line is important which is located at $4\omega_1$.

A treatment similar to that in [10] for $I = 5/2$ is presented here for spin $7/2$. It provides the starting point for spin-echo studies [11] and a detailed analysis of the nutation frequencies and intensities for such systems.

References

- [1] SAMOSON, A., and LIPPMAA, E., 1988, *J. magn. Reson.*, **79**, 255.
- [2] SAMOSON, A., and LIPPMAA, E., 1983, *Phys. Rev. B*, **28**, 6567.
- [3] GOLDMAN, M., 1990, *Adv. magn. opt. Reson.*, **14**, 59.
- [4] SANCTUARY, B. C., and HALSTEAD, T. K., *Adv. magn. opt. Reson.*, **15**, 79.
- [5] MAN, P. P., 1991, *Molec. Phys.*, **72**, 321.
- [6] MAN, P. P., 1992, *Molec. Phys.*, **76**, 1119.
- [7] HARRIS, R. K., and LESBITT, G. J., 1988, *J. magn. Reson.*, **78**, 245.
- [8] WOKAUN, A., and ERNST, R. R., 1977, *J. chem. Phys.*, **67**, 1752.
- [9] LEE, N., SANCTUARY, B. C., and HALSTEAD, T. K., 1992, *J. magn. Reson.*, **98**, 534.
- [10] MAN, P. P., 1993, *Molec. Phys.*, **78**, 307.
- [11] MAN, P. P., 1994, *Z. Naturf. A*, **49**, 89.
- [12] WOKAUN, A., and ERNST, R. R., 1977, *J. chem. Phys.*, **67**, 1752.
- [13] VEGA, S., 1978, *J. chem. Phys.*, **68**, 5518.